33RD CONGRESS
OF THE INTERNATIONAL COUNCIL
OF THE AERONAUTICAL SCIENCES
STOCKHOLM, SWEDEN, 4-9 SEPTEMBER, 2022

ICAS 2022 SWEDEN

CONTROL AUGMENTATION SYSTEM DESIGN FOR THE QUAD TILT-WING UAV VIA H_∞ STRUCTURE WITH GWO

Kranthi Kumar Deveerasetty[1], Koichi OKA[1] & Akinori HARADA[1]

[1]Department of Intelligent Mechanical Engineering, School of System Engineering, Kochi University of Technology, Japan 782-8502

Abstract

In this paper, an approach based on H_∞ is proposed, in which reasonable bounds is employed and Grey wolf optimization is used to design the Control Augmentation System (CAS) for a Quad Tilt-Wing Unmanned Aerial Vehicle (QTW-UAV). Grey Wolf Optimization (GWO) is used to find the global optimal proportional-integral gains via H_∞ structure. The CAS controller gains has been computed for a QTW-UAV from H_∞ criteria. Simulation results are presented to show the validation of the technique.

Keywords: Control Augmentation System, Quad Tilt-Wing, Unmanned Aerial Vehicle, Grey Wolf Optimization

1. Introduction

Quad-Tilt-Wing (QTW) unmanned aerial vehicle (UAV) is a hybrid vehicle and it has the capability to operate as a VTOL and high speed cruse performance. The main advantage of the QTW-UAV does not require any runway compared with the fixed wing UAV. The Japan Aerospace Exploration Agency (JAXA) has successfully developed a series of prototype QTW-UAVs such as QUX-02A [1], AKITSU [7] and McART3 [8]. The QTW-UAV has four propellers installed at the center of the front and rear wings and the thrust directions vary from 0deg to 90deg by tilting the both wings simultaneously. The dynamics of the QTW-UAV varies at different titling angle of the wings and designing a flight controller is a quite challenging. The flight controller design is a crucial element to guarantee the safety of the QTW-UAV because both longitudinal and later-directional dynamic characteristics are unstable for the majority the tilt-wing angles. To overcome this complication, the various flight controllers are designed [1] - [4]. The QTW-UAV has advantages over the tilt rotor in terms of aerodynamic characteristics in both hover and cruise. Because tilting wings do not disturb the propeller slip streams in the hover and thus produce large lift, a long wingspan and winglets can be used to reduce induced drag (particularly in cruise). Tilt wing and tilt rotor vehicles gain the benefits of both fixed-wing aircraft and helicopters. Changing wing or rotor tilt angles cause significant changes in aerodynamic characteristics. The attitude control system was designed using a Kalman filter-based linear quadratic integral (LQI)control approach [3]. Sabanci University in Turkey has created the "SUAVI" QTWUAV [4]. They have achieved virtually complete conversion flight (up to 15 degrees) in physical situations. They may have achieved full flight, but full conversion from helicopter to aircraft mode has yet to be recorded, according to the authors. SUAVI's most efficient tilt angle is approximately 15.0 degrees, thus it doesn't need to be completely converted The SCAS structure was pre-designed, and the controller gains were left as configurable parameters. The robustness criterion was addressed in the design process by ensuring robust stability and performance against a collection of models with a finite number of models at the nominal configuration. The multiple-model approach is the name for this method [2]. Researchers of [5], [6] and [7] were successful in building a gain-scheduled PI controller for an AKITSU QTW UAV capable of complete conversion flying from helicopter to aircraft mode. Japanese researchers Sato and Muraoka [8] created a gain-scheduled PI controller for a QTW UAV- McART3. They specified seven preset wing tilt angles ranging from 90 degrees to 0 degrees.

Control action moderation was achieved by limiting the search space of controller gain values during the design stage. The QTW-UAV flight controller was tested successfully in a conversion flight [8]. However, oscillatory motions occur in both longitudinal and lateral motions. Similar signals were identified during McART3's flight test [8]. The oscillatory activity in the lateral-directional movement, in particular, was sometimes extensive and should thus be suppressed for flight safety.
Totoki et al [9]. proposed two low-order controller design approaches by expanding current linear matrix inequality (LMI)-based control design and model order reduction (MOR) methods and demonstrated their applicability by creating flight controllers for McART3. Based on the H_∞ framework, [11] proposes an alternative approach to QTW-UAV SCAS design; this approach considers controller structure constraints as in [8] and solves the optimization problem using particle swarm optimization (PSO) [12]. Performance requirements are given in the frequency domain and formalized as weighting functions in this approach, and the multiple-model method is used to achieve robustness, i.e., again yielding a necessary robustness condition. Tran et al. [10] enhanced the transition behavior of a quadrotor-tilt-wing VTOL aircraft employing a robust control augmentation system and affirmed their design on an actual vehicle. A nonparametric inverse multiplicative uncertainty description accounts for the uncertainties of the aircraft attitude dynamics at each operating state, with particular attention to fluctuations in the number of unstable modes. The resultant μ-synthesis problem with a frequency-dependent weighting function, the structure of which is known in advance, is restated as a H_∞-structured problem and solved using MATLAB software [13].
This study aims to create a simple and computationally efficient CAS tuning technique for robust PI controllers that meet H_∞ requirements. The typical strategies for determining such controller improvements are computationally complex. As a result, to tackle such a design challenge quickly and directly without requiring any sophisticated manipulations, we adopted the Grey Wolf Optimization (GWO) problem [14]. However, if a complicated CAS is used to improve control performance, there may be an issue. We present a design strategy with frequency domain limitations produced by decreasing computational complexity for optimization; that is, the CAS benefits are designed by shaping the sensitivity function inside the H_∞ framework to address the shortcomings, as mentioned earlier.

2. Quad-Tilt-Wing UAV

The QTW works in a range of wing tilt angles τ_w from 90 degrees (helicopter mode) to 0 degrees (aircraft mode); moreover, a so-called CLEAN (i.e., cruise) operating mode is established at τ_w 0 degrees, with flaps retracted to optimize airplane mode efficiency. The set of wing tilt angles analyzed is the same as [8]. Wing tilting is employed to regulate the operational state of the vehicle, such as landing gears and traditional flaps, rather than for control. A discrete set of numbers allows the pilot to pick the desired wing tilt angle manually. Table 1 summarizes the operating circumstances studied in this research; the tilt-wing angleτ_w defines the operating condition. Each operating state has a true airspeed (TAS) connected, which is also provided in the table.

2.1 CAS Design for the QTW-UAV

The block diagram of the longitudinal QTW-UAV is shown in Figure 1. In helicopter mode, the pitch control is generated by the difference of thrust between the fore and rare propellers. In airplane mode, the pitch control is generated by the difference of force made by the fore and rare flaperons. The optimized stability augmentation system (SAS)gain values are unitized from JAXA [8]. The CAS uses proportional and integral (PI) gains as a feedback controller for the tracking of the pitch command.

2.2 Robust CAS PI Controller Tuning Strategy

The classical PI controller is given as

$$C(s) := \frac{K_p s + K_i}{s} \tag{1}$$

where K_p is the proportional gain and K_i is the integral gain. The classical loop-shaping method for determining the magnitude of the open-loop transfer function $L(s) = G(s)C(s)$. In contrast, closed-loop transfer functions, such as Sensitivity function $\left((S(s;x)) = \frac{1}{1+G(s)C(s;x)}\right)$, which influence the final

Table 1 – QTW-UAV design models and perturbed models with operating points

Design point	Model Name	Tilt-angle	TAS
T(90)	τ_{wn1}[90]-N (nominal)	90	1.0
	τ_{wp1}[80]-P1 (perturbed)	80	2.5
	τ_{wp2}[70]-P2 (perturbed)	70	5.0
T(70)	τ_{wn2}[70]-N (nominal)	70	5.0
	τ_{wp1}[80]-P1 (perturbed)	80	2.5
	τ_{wp2}[60]-P2 (perturbed)	60	7.0
T(50)	τ_{wn3}[50]-N (nominal)	50	8.0
	τ_{wp1}[60]-P1 (perturbed)	60	7.0
	τ_{wp2}[40]-P2 (perturbed)	40	9.5
T(30)	τ_{wn4}[30]-N (nominal)	30	11.0
	τ_{wp1}[40]-P1 (perturbed)	40	9.5
	τ_{wp2}[20]-P2 (perturbed)	20	13.0
T(15)	τ_{wn5}[15]-N (nominal)	15	14.0
	τ_{wp1}[20]-P1 (perturbed)	20	13.0
	τ_{wp2}[10]-P2 (perturbed)	10	14.5
T(0)	τ_{wn5}[0]-N (nominal)	0	19.0
	τ_{wp1}[10]-P1 (perturbed)	10	14.5
	τ_{wp2}[CLEAN]-P2 (perturbed)	CLEAN	24.0
T(CLEAN)	τ_{wn6}[CLEAN]-N (nominal)	ClEAN	24.0
	τ_{wp1}[00]-P1 (perturbed)	0	19.0

response, are not considered directly. The controller designed can be expressed as an H_∞ constraint optimal performance. The function of sensitivity $(S(s;x))$ is an excellent predictor of closed-loop performance in both SISO and MIMO systems. The main advantage of considering sensitivity function is that, because we ideally want sensitivity function to be small, we only need to consider its magnitude of the $(S(s;x))$; we don't need to worry about its phase. The aim of the article is to satisfy the following condition

$$\min_{x} \max_{N\&P\text{models}} \|W(j\omega)S(j\omega;x)\|_\infty < 1, \forall\omega \tag{2}$$

where $W(s)$ is the weighting function and the required. If the above constraint contented, then the sensitivity function $|S(j\omega;x)| < \frac{1}{W(j\omega)}, \forall\omega$ and the above equation derives from the definition of H_∞ norm. The weighting function that represent the required levels of stability and performance.

2.3 Grey Wolf Optimization (GWO)

The traditional Grey wolf optimization (GWO) method introduced by Mirajalili et al. [14] is briefly described in this section. Grey wolf optimization (GWO) is a meta-heuristic optimization technique and it has many advantages such as simplicity, derivative-free mechanism, flexibility and had an ability to avoid local optimal value. The algorithm inspired from the animals behaviour. To find the optimum value there is no to calculate the derivative of the search space. GWO algorithm has stochastic nature and has an ability to search the entire search region to find the best optimization values. The basic algorithm of the GWO are as follows [14]

- The prey is being tracked, chased, and approached.
- The second step is pursue the victim, encircle it, and annoy it until the prey stops moving..
- Finally, attacking the prey.

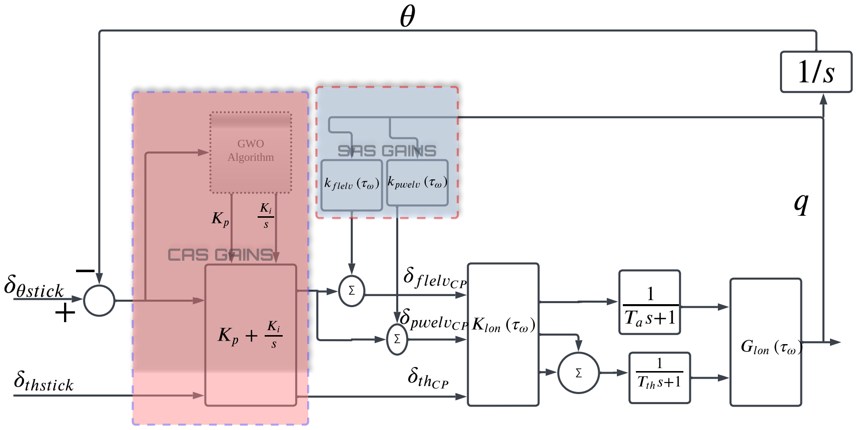

Figure 1 – Block diagram for the longitudinal motions of the QTW-UAV [6]

The mathematical model of the GWO optimization algorithm consists of various types of solutions and the best solution as the alpha (α). The second best solution is known as beta (β) and the third best solution is known as delta (δ). The remaining solutions are named as omega (ω) and update encircling positions of the (α), (β), and (δ).

$$\vec{\mathrm{D}} = \left|\vec{\mathrm{C}} \cdot \vec{\chi}_p(t) - \vec{\chi}(t)\right| \tag{3}$$

$$\vec{\chi}(t+1) = \vec{\chi}_p(t) - \vec{\mathrm{A}} \cdot \vec{\mathrm{D}} \tag{4}$$

where $\vec{\mathrm{C}} = 2 \cdot \vec{r}_2$, $\vec{\mathrm{A}} = 2\vec{\mathrm{a}} \cdot \vec{r}_1 - \vec{\mathrm{a}}$, t is the current iteration, $\vec{\chi}_p$ is the prey position vector, $\vec{\chi}$ is the grey wolf position vector, $\vec{\mathrm{a}}$ is diminish gradually from 2 to 0, and the random numbers r_1, r_2 are $[0,1]$. In the process of optimization, the updated encircling positions of the (α), (β), and (δ) is done by the ω wolf as follows:

$$\begin{aligned} &\vec{\mathrm{D}}_\alpha = \left|\vec{\mathrm{C}}_1 \cdot \vec{\chi}_\alpha - \vec{\chi}\right|, \vec{\mathrm{D}}_\beta = \left|\vec{\mathrm{C}}_2 \cdot \vec{\chi}_\beta - \vec{\chi}\right|, \\ &\vec{\mathrm{D}}_\delta = \left|\vec{\mathrm{C}}_3 \cdot \vec{\chi}_\delta - \vec{\chi}\right| \end{aligned} \tag{5}$$

$$\begin{aligned} &\vec{\chi}_1 = \vec{\chi}_\alpha - \vec{\mathrm{A}}_1 \cdot \left(\vec{\mathrm{D}}_\alpha\right), \vec{\chi}_2 = \vec{\chi}_\beta - \vec{\mathrm{A}}_2 \cdot \left(\vec{\mathrm{D}}_\beta\right), \\ &\vec{\chi}_3 = \vec{\chi}_\delta - \vec{\mathrm{A}}_3 \cdot \left(\vec{\mathrm{D}}_\delta\right), \end{aligned} \tag{6}$$

$$\vec{\chi}(t+1) = \frac{\vec{\chi}_1 + \vec{\chi}_2 + \vec{\chi}_3}{3} \tag{7}$$

where the current position is defined by the $\vec{\chi}$, the random vectors are denoted as $\vec{\mathrm{C}}_1$, $\vec{\mathrm{C}}_2$ and $\vec{\mathrm{C}}_3$, the positions of the α, β, and δ are named as $\vec{\chi}_\alpha$, $\vec{\chi}_\beta$, and $\vec{\chi}_\delta$.

3. QTW-UAV Simulation Results

We obtained the CAS gains using the proposed methods, and the gain values are given in Tables Table 2 and Table 3. In the longitudinal motion, except at the CLEAN angle, the obtained optimized gain values are the same as the results published by Sato and Muraoka [8]. Our obtained gain values are also compared with the results given by Nami et al., [11], and reported gain values are different at Tilt angles 70 deg, 15 deg, and CLEAN. The Weight selection $W_s$is chosen with the MATLAB command "makeweight" function as the low-pass filter, whose features are specified with three parameters: DC gain, ω, and High-Frequency (HF) gain. The DC gain value is chosen $1.0 * 10^{-6}$. The ω gains are obtained by the trail-an-error method and the HF gains are then set to be very near to the closed-loop sensitivity function's highest peak gains. For more details please refer [8] and [12]. In Table 3, the obtained optimized gain values are different from the existing literature. The step response for the nominal 15 deg is shown in Figure 2. The step response for the 15 deg perturbed models are depicted in Figure 3 and Figure 4. The responses for the 70 deg and clean are shown from Figure 8 to Figure 9. We tried to reduce the oscillation but the changes are minor. In the lateral-directional motion, the obtained optimized gain values are different then the results published by Sato and Muraoka [8], [11], and [12]. The responses for the 30 deg are depicted in Figure 10, Figure 11, and Figure 12. From the responses, it is clear that the proposed technique is acceptable and it is cable of reducing oscillations but the response of the controller is little slow.

Table 2 – Design of CAS gains for longitudinal-directional motions

Design point	K_p	K_i	K_p (GWO)	K_i (GWO)	K_p [11]	K_i [11]	K_p [8]	K_i [8]	ω(rad/sec)	HF
T(90)	$[-50,0]$	$[-40,0]$	–	–	–	–	–	–	-	-
T(70)	$[-50,0]$	$[-40,0]$	-50	-40	-49	-20	-50	-40	0.97	5.5
T(50)	$[-100,0]$	$[-50,0]$	-100	-70	-100	-67	-100	-70	0.4	1.75
T(30)	$[-150,0]$	$[-100,0]$	-150	-100	-150	-100	-150	-100	0.3	1.9
T(15)	$[-150,0]$	$[-100,0]$	-150	-100	-146	-92	-150	-100	0.3	1.9
T(0)	$[-100,0]$	$[-100,0]$	-100	-100	-100	-98	-100	-100	0.95	2.6
cln	$[-70,0]$	$[-70,0]$	-42.5497	-2.5	-43	-2	-70	-33	0.9	1.1

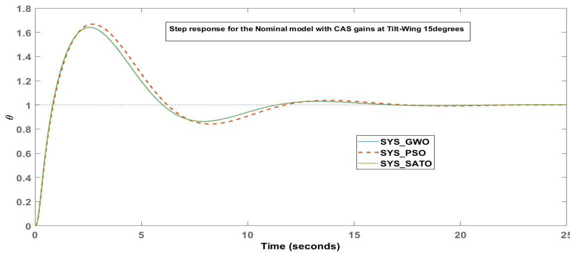

Figure 2 – Step response of closed-loop systems for nominal model at 15deg (longitudinal motion)

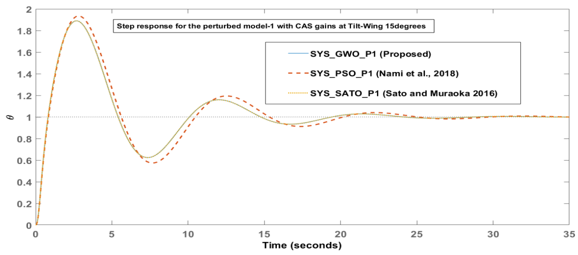

Figure 3 – Step response of closed-loop systems for perturbed-1 model at 15deg (longitudinal motion)

Table 3 – Design of CAS gains for lateral-directional motions

Design point	K_p	K_i	K_p (GWO)	K_i (GWO)	K_p [11]	K_i [11]	K_p [8]	K_i [8]	K_p [12]	K_i [12]	ω(rad/sec)	HF
T(90)	$[-50,0]$	$[-40,0]$	-25.8473	-31.1090	-50	-40	-44	-40	-38	-34	0.3	1.5
T(70)	$[-50,0]$	$[-40,0]$	-15.6101	-14.6944	-50	-40	-27	-39	-40	-37	0.6	1.5
T(50)	$[-80,0]$	$[-50,0]$	-6.2258	-10.9601	-80	-50	-64	-50	-41	-19	1.7	1.6
T(30)	$[-120,0]$	$[-50,0]$	-23.6084	-20.9286	-88	-50	-106	-48	-41	-19	2	3
T(15)	$[-100,0]$	$[-100,0]$	-22.5153	-26.4330	-100	-50	-79	-50	-42	-26	0.6	2
T(0)	$[-100,0]$	$[-50,0]$	-55.2038	-44.5632	-100	-50	-94	-48	-55	-45	0.65	3
cln	$[-70,0]$	$[-70,0]$	-27.9126	-19.4182	-100	-50	-94	-50	-31	-22	2	2

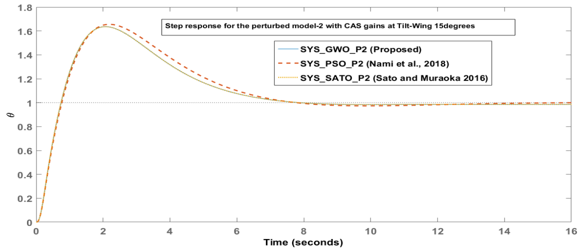

Figure 4 – Step response of closed-loop systems for perturbed-2 model at 15deg (longitudinal motion)

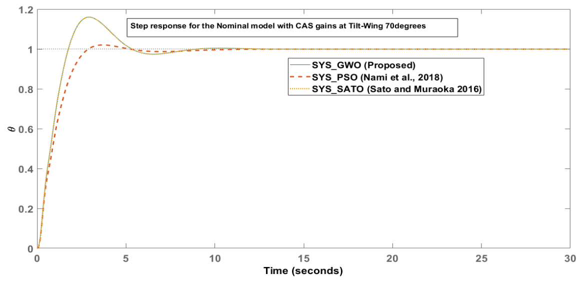

Figure 5 – Step response of closed-loop systems for nominal model at 70deg (longitudinal motion)

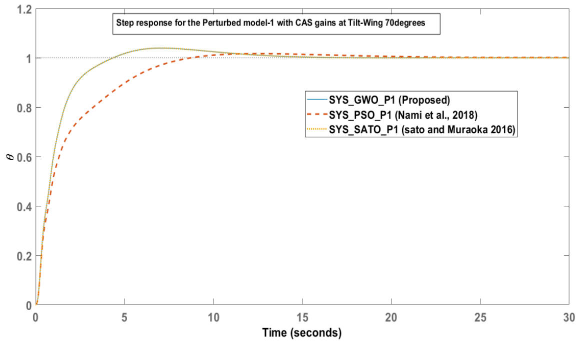

Figure 6 – Step response of closed-loop systems for perturbed-1 model at 70deg (longitudinal motion)

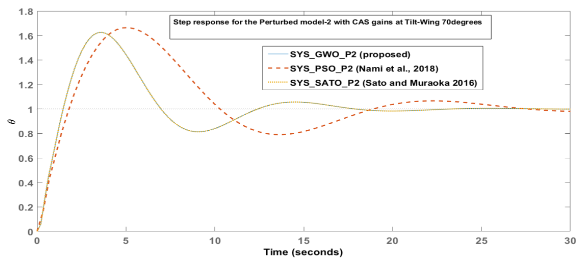

Figure 7 – Step response of closed-loop systems for perturbed-2 model at 70deg (longitudinal motion)

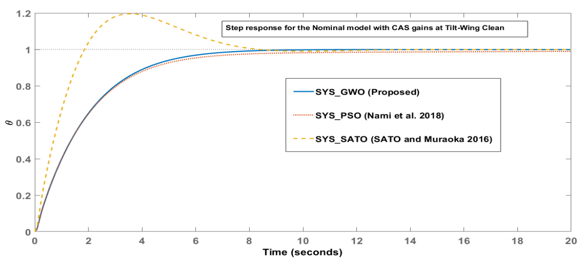

Figure 8 – Step response of closed-loop systems for Nominal model at CLEAN deg (longitudinal motion)

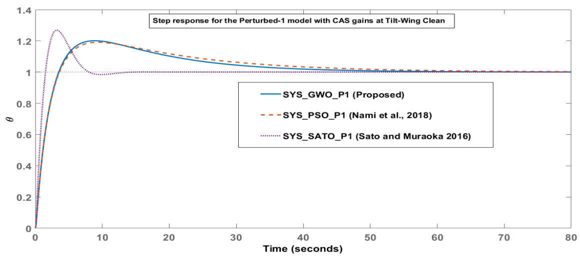

Figure 9 – Step response of closed-loop systems for perturbed-2 model at CLEAN deg (longitudinal motion)

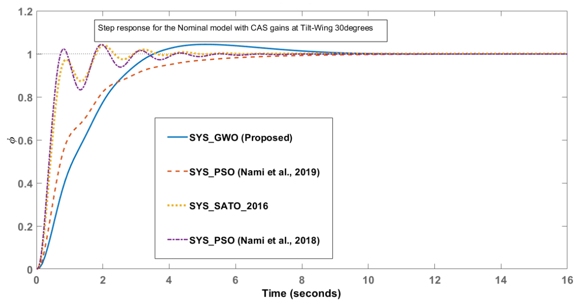

Figure 10 – Step response of closed-loop systems for Nominal model at 30 deg (lateral motion)

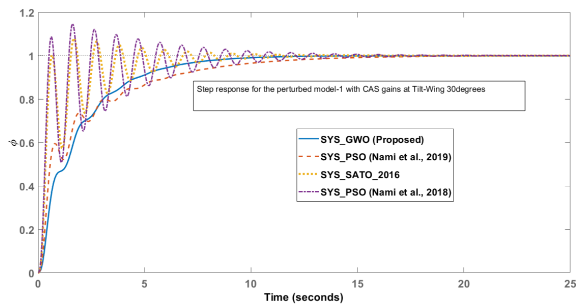

Figure 11 – Step response of closed-loop systems for perturbed-1 model at 30 deg (lateral motion)

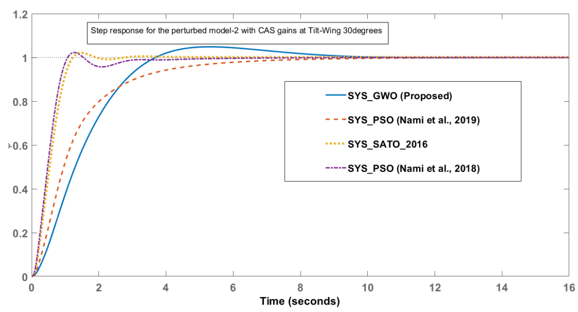

Figure 12 – Step response of closed-loop systems for perturbed-2 model at 30 deg (lateral motion)

4. Conclusions

This paper proposes the GWO optimized PI controller for the CAS of the QTW-UAV. The simulation results are compared with the existing techniques. For the error of the closed-loop system using the weighted sensitivity function, the proposed method must satisfy the H_∞ norm constraint. The obtained results are satisfactory for the lateral directional motion. Still, the results need to be better for the longitudinal movement to suppress the oscillation motion. The cause of oscillation is due to fixed-order controller design.

5. Contact Author Email Address

Kranthi Kumar Deveerasetty: kranthi.kumar@kochi-tech.ac.jp

6. Copyright Statement

References

[1] Muraoka K, Okada N and Kubo. D. Quad tilt wing VTOL UAV: Aerodynamic characteristics and prototype flight test. *AIAA Infotech@Aerospace Conference*, Seattle, Washington, USA, pp 1-10, 2009.

[2] Ackerman J. *Multi-Model approaches to robust control system design*. Uncertainty and Control, Lecture Notes in Control and Information Sciences, Springer, Berlin, Vol. 70, pp 108-130, 2001.

[3] Suzuki S, Zhijia R, Horita Y, Nonami K, Kimura G, Bando T, Hirabayashi D, Furuya M and Yasuda K. Attitude control of quad rotors QTW-UAV with tilt wing mechanism. *Journal of System Design and Dynamics*, Vol. 4, No.3, pp 416-428, 2010.

[4] Cetinsoy E, Dikyar S, Hancer C, Oner K. T, Srimoglu E, Unel M and Aksit M. Design and construction of a novel quad tilt-wing UAV. *Mechatronics*, Vol. 22, No.6, pp 723-745, 2012.

[5] Muraoka K, Okada N, Kubo D, and Sato M. Transtion flight of quad tilt wing VTOL UAV. 28^{th} *International Congress of the Aeronautical Sciences*, Brisbane, Australia, pp 1-10, 2012.

[6] Sato M and Muraoka K. Flight test verification of flight controller for quad tilt wing unmanned aerial vehicle. *AIAA Guidance Navigation, and Control (GNC) Conference*, Boston, MA, pp 1-17, 2013.

[7] Sato M and Muraoka K. Flight controller design and demonstartion of quad-tilt-wing unmanned aerial vehicle. *Journal of Guidance, Control, and Dynamics*, Vol. 38, No. 6, pp 1071-1082, 2015.

[8] Sato M and Muraoka K. Flight controller design for small quad tilt wing uav. *Journal of the Japan Society for Aeronautical and Space Sciences*, Vol. 64, No. 1, pp 79-82, 2016. (in Japanese)

[9] Totoki H, Ochi Y, Sato M and Muraoka K. Design and testing of a low-order flight control system for quad-tilt-wing UAV. *Journal of Guidance, Control, and Dynamics*, Vol. 39, No. 3, pp 2423-2430, 2016.

[10] Tran A.T, Sakamoto N, Sato M, and Muraoka K. Control augmentation system design for quad-tilt-wing unmanned aerial vehicle via robust output regulation method. *IEEE Transactions on Aerospace and Electronic Systems*, Vol. 53, No. 1, pp 357-369, 2017.

[11] Nami C, Oka K, Harada A, and Sato M. H_∞ control-based design of QTW-UAVs using particle swarm optimization. *Journal of the Japan Society for Aeronautical and Space Sciences*, Vol. 61, No. 5, pp 226-229, 2018.

[12] Nami C, Oka K, Sato M, Harada A, and Muraoka K. H_∞ control-based robust CAS design for QTW-UAVs via multiple-model approach with particle swarm optimization. *International Journal of Aerospace Engineering*, pp. 1-17, 2019.

[13] Panza S, Lovera M, Sato M, and Muraoka K. Structured μ-synthesis of robust attitude control laws for quad-tilt-wing unmanned aerial vehicle, *Journal of Guidance, Control, and Dynamics*, Vol.43, No. 12, pp 1-17, 2020.

[14] Mirjalili S, Mirjalili S. M and Lewis A. Grey wolf optimizer. *Advances in Engineering Software*, Vol.69, pp 46-61, 2014.